Available online at www.sciencedirect.com
SCIENCE DIRECT®
Tetrahedron: Asymmetry
Tetrahedron: *Asymmetry* 15 (2004) 1607–1613

Composition and structure of activated complexes in stereoselective deprotonation of cyclohexene oxide by a mixed dimer of chiral lithium amide and lithiated imidazole

Daniel Pettersen, Peter Dinér, Mohamed Amedjkouh and Per Ahlberg*

Department of Chemistry, Göteborg University, SE-41296 Göteborg, Sweden

Received 8 March 2004; accepted 29 March 2004

Abstract—Stereoselective deprotonation of cyclohexene oxide, using a mixed dimer built of the chiral lithium amide, lithium (1*R*,2*S*)-*N*-methyl-1-phenyl-2-pyrrolidinyl-propanamide, and 2-lithio-1-methylimidazole, has been studied. The composition of the rate limiting activated complex was determined by kinetics to be built from one mixed dimer molecule and one epoxide molecule. Based on this knowledge computational chemistry has been applied to gain insight into possible structures of the activated complexes.

1. Introduction

Chiral lithium amides have been developed for enantioselective deprotonation reactions of, for example, epoxides and ketones.[1] Such reactions are synthetically important since the chiral products obtained are useful intermediates in the organic synthesis, for example, of biologically active compounds.[2] The chiral lithium amides are often applied in stoichiometric amounts or in excess. Alternatively, there have also been a number of attempts to run the enantioselective deprotonation reactions, for example, of epoxides under catalytic conditions.[2–4] The chiral lithium amide (R*NLi) has been used in sub-stoichiometric amounts in the presence of a bulk base (BLi) working as a chiral lithium amide-regenerating reagent, in order to obtain a catalytic cycle (Scheme 1). However, nonenantioselective deprotonation by the bulk base yields a racemic product that competes with that of the chiral base, resulting in lower enantioselectivity than in the stoichiometric reaction with chiral lithium amide.

In order to improve the degree of enantioselectivity in catalytic deprotonations, access to bulk bases with lower kinetic basicity than, for example, lithium diisopropyl lithium amide LDA, but with comparable or higher thermodynamic basicity, is required. In our search for such bases, we used 1-methylimidazole **1** as a bulk base precursor.[4,5] This azole underwent carbon deprotonation at the C-2-position by *n*-BuLi to yield the carbenoid compound 2-lithio-1-methylimidazole Li-**1** (Scheme 2).[5,6]

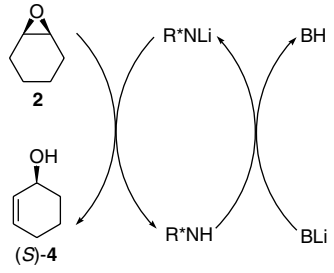

Scheme 1.

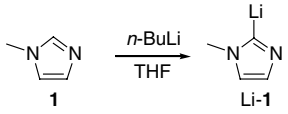

Scheme 2.

The deprotonating ability of the base Li-**1** was studied using cyclohexene oxide **2** as substrate. In contrast to LDA, Li-**1** did not yield any deprotonation of **2**. This is

* Corresponding author. Tel.: +46-31-772-2899; fax: +46-31-772-2908; e-mail: per.ahlberg@chem.gu.se

0957-4166/$ - see front matter © 2004 Elsevier Ltd. All rights reserved.
doi:10.1016/j.tetasy.2004.03.042

presumably due to the fact that proton transfer to carbon is usually slower than that to a more electronegative atom such as nitrogen. This result indicates that Li-**1** should be a useful bulk base in catalytic asymmetric deprotonation.

Indeed as expected, it was found that when using Li-**1** as a bulk base instead of LDA together with the chiral base Li-**3** as a catalyst, deprotonation of **2** produced chiral allylic lithium alkoxide (*S*)-Li-**4** with the same reproducible stereoselectivity (93% ee) as the deprotonation in the absence of the bulk base.[4]

Interestingly, when running the deprotonation using equimolar amounts of chiral base Li-**3** and bulk base Li-**1** an increase in stereoselectivity (96% ee) was observed. Apparently the bulk base plays a more intricate role than just regenerating the chiral base from the chiral diamine formed upon deprotonation of the epoxide.[4]

We herein report the results of an investigation into molecular composition of the deprotonation activated complexes. Kinetics have been used to determine the composition of the rate limiting activated complexes and based on this knowledge, computational chemistry has been applied to calculate structures of the activated complexes.

2. Results and discussion

Kinetics can tell us about the molecular composition of activated complexes in reactions through experimentally determined reaction orders, if the molecular composition of the reagents in the initial state is known.[7]

Lithium amides are strong dipoles, which makes them prone to aggregate.[8] The aggregate composition of homochiral lithium amide Li-**3** has previously been investigated using ^{6}Li and ^{13}C labeled chiral lithium amide and multinuclear NMR spectroscopy.[5] The results show that Li-**3** in tetrahydrofuran (THF) is present as homodimer (Li-**3**)$_2$ in the initial state (Scheme 3).

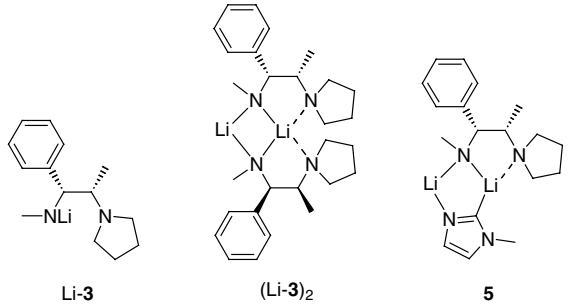

Li-**3** (Li-**3**)$_2$ **5**

Scheme 3.

The rate-limiting activated complex in the deprotonation reaction of epoxide **2** by (Li-**3**)$_2$ has been shown to be built from one molecule of **2** and one molecule of (Li-**3**)$_2$ rather than a monomer of Li-**3**.[7,9] Furthermore, by using mixtures of isotopically labeled Li-**3** and Li-**1**, it was shown that mixed dimer (heterodimer) **5**, composed of one molecule of Li-**1** and one molecule of Li-**3**, is formed. In solutions made from equimolar amounts of Li-**1** and Li-**3** in THF, heterodimer **5** was exclusively formed at the expense of homoaggregates (Scheme 3).

In order to clarify the role of the mixed dimer in the deprotonation reaction, we performed kinetic and computational studies of the composition and structures of the rate-limiting activated complexes involved in the reaction.

The asymmetric deprotonation of cyclohexene oxide **2** by mixed dimer **5** was carried out in THF at 20.0 °C using different concentrations of **2** and **5**. The concentrations of product **4** over time were determined using a calibrated quench-extraction-GC procedure. The reactions were followed close to completion; a plot of the concentration of the product versus time turned out to be close to linear for a large fraction of the reaction. This indicated that the reaction products diamine (1*R*,2*S*)-*N*-methyl-1-phenyl-2-pyrrolidinyl-propanamide **3** and 1-methylimidazole **1** modify the rates of the reactions. The enantiomeric excess of the (*S*)-allylic alcohol was found not to change significantly (±0.2%) during the reaction. In order to avoid interference of reaction products, initial rates were determined using data for only ca. 0.5% conversion (Table 1).

Table 1. Initial rates obtained from 0.5% reaction in runs with different concentrations of reagents and additives in THF at 20.0 °C

Run	[**2**]/mM	[**5**]/mM	[(Li-**3**)$_2$]/mM[a]	[**1**]/mM	[**3**]/mM	(d[**4**]/dt)/10^{7} M s^{-1}
	50	100				11.5
	50	100				11.4
	50		100			51.3[a]
	100	50				11.8
	100	50				11.8
	100	75				18.1
	100	75				18.7
	100	100				22.4
	100	100				23.2
	100	100				23.1
	100	100				23.0
	100	100		100		13.5
	100	100			100	58.5
	100		100			103[a]
	100		100			102[a]
	100	200				41.0
	100	200				46.9
	200	100				47.4
	200	100				48.9
	200		100			195[a]

[a] Initial rates taken from Ref. 9.

The reaction orders with respect to the epoxide **2** and the mixed dimer **5** were obtained from the plots of log (initial rate) versus log (concentration) as shown in Figures 1 and 2.

The gradients give the experimental reaction orders and were determined to be 1.03 and 0.94 for **2** and **5**,

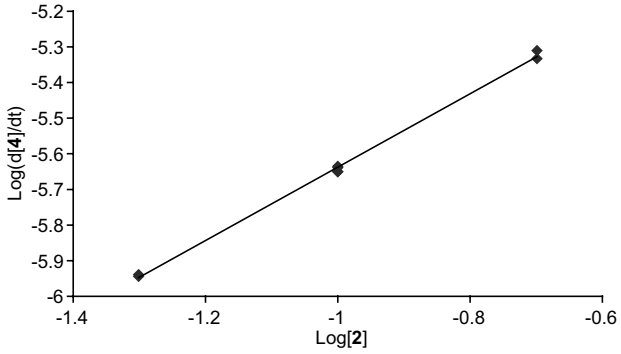

Figure 1. Plot of log(d[**4**]/dt) versus log[**2**] is shown and the reaction order with respect to **2** obtained from the gradient.

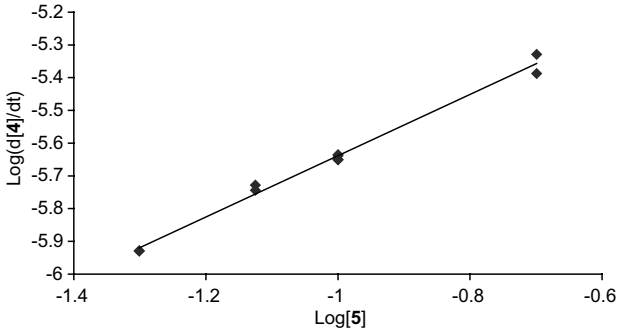

Figure 2. Plot of log(d[**4**]/dt) versus log[**5**] is shown and the reaction order with respect to **5** obtained from the gradient.

respectively, that is, the reaction is first-order both in the case of the epoxide **2** and mixed dimer **5**. This shows that the deprotonation takes place via a transition state built from one molecule of epoxide **2** and one molecule of heterodimer **5**. This is in contrast to the results of the kinetics in THF for the deprotonation of **2** by (Li-**3**)$_2$ in the absence of Li-**1**, which has previously shown that the transition state is composed of one molecule of homodimer (Li-**3**)$_2$ and one molecule of epoxide **2**.[9] This difference in transition state composition is concluded to be the reason for the change of stereoselectivity. The difference between the stereoselectivities observed for the reactions run under stoichiometric conditions (96% ee) and catalytic conditions (93% ee) could be due to differential solvation by the lithium methylimidazole of the diastereoisomeric activated complexes. This acquired knowledge of the molecular composition of the activated complexes was the starting point for a computational investigation of possible activated complex structures with the results presented below.

3. Computational studies of the activated complexes

The potential energy surfaces for the stereoselective deprotonations were explored computationally. The rate limiting activated complexes were identified as the deprotonation activated complexes. The geometries and energies of possible isomeric activated complexes leading to (*R*)- and (*S*)-products have been calculated. Initially, the PM3 level of theory[10–14] was used, since PM3 is known to give geometries of organolithium compounds similar to those obtained from experiment and high level theory.[15,16] The most stable structures were optimized using density functional theory (DFT). In the calculations of the deprotonation activating complex involving heterodimer **5**, a *syn*-β-elimination mechanism was assumed.[17,18] Recently, experimental evidence for this mechanism has been obtained.[19] Calculations of heterodimer **5** itself have previously been reported.[5]

In the transition states for deprotonation of **2**, one lithium atom (Li1) from the mixed dimer coordinates to the epoxide oxygen (O1), while the amide nitrogen (N1) abstracts the β-proton (Scheme 4).

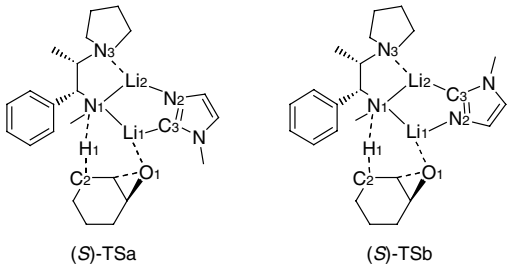

Scheme 4.

The most stable unsolvated activated complexes, leading to (*R*)- and (*S*)-product at the B3LYP/6-31 + G(d)//PM3 level of theory, were further optimized at B3LYP/6-31G(d)//B3LYP/6-31G(d) level of theory.[20,21] The most stable activated complexes, (***R***)-**TSa** and (***S***)-**TSa**, have an (*R*)-configuration on the amide nitrogen (N1) while the oxygen-coordinated lithium atom (Li1) was also coordinated to the carbon (C3) in the imidazole ring (Fig. 3).

All distances in the reaction center six-membered rings of the activated complexes (***R***)-**TSa** and (***S***)-**TSa** are similar (Fig. 3). The C1–O1 bond of the epoxide part was substantially broken (1.97 Å), while the N1–Li1 coordination in the activated complexes were elongated (2.14 Å) when compared to the Li1–N1 coordination bond in the mixed dimer itself (1.91 Å). Geometrical differences between the diastereoisomeric activated complexes (***R***)-**TSa** and (***S***)-**TSa** were found in the orientation of the phenyl group and of the methyl group attached to the amide nitrogen (N1). In (***R***)-**Tsa**, the phenyl group is located on the same side of the mixed dimer as the cyclohexene oxide moiety while the *N*-methyl group is on the opposite side. In (***S***)-**TSa**, the *N*-methyl group is located on the same side as the cyclohexene oxide moiety while the phenyl group is on the opposite side.

The next most stable activated complexes at the B3LYP/6-31 + G(d)//PM3 level of theory, (***R***)-**TSb**, and (***S***)-**TSb**, were also further optimized at B3LYP/6-31G(d) level of theory. In these activated complexes, the oxygen-coordinated lithium coordinates to the nitrogen (N2) in the

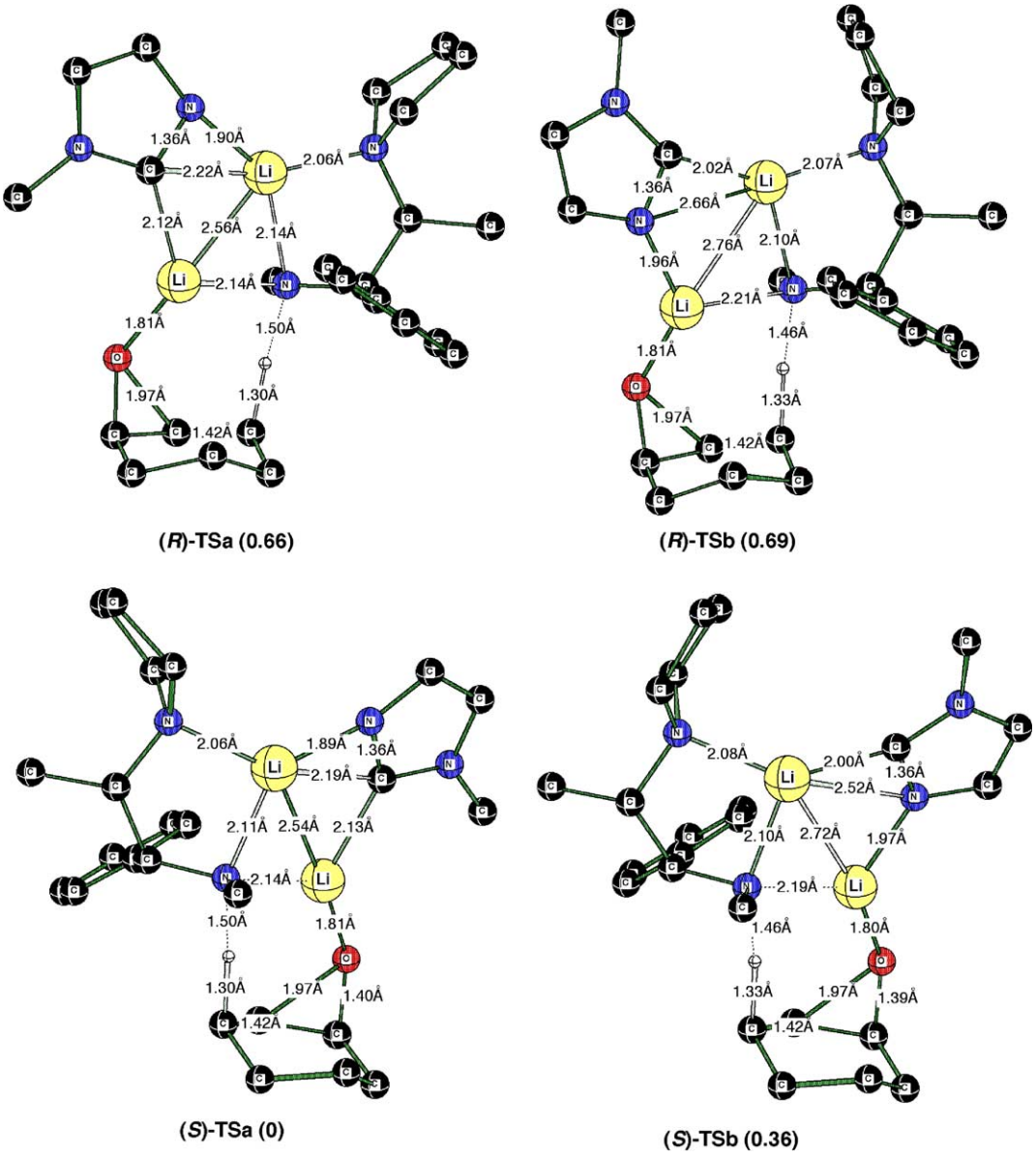

Figure 3. Optimized unsolvated activated complexes at B3LYP/6-31G(d) level of theory. Relative energies in kcal mol^{-1} are shown in parentheses. Hydrogens are omitted for clarity.

imidazole ring rather than C3. The different orientation of the imidazole ring in activated complexes, (***R***)-**TSb**, and (***S***)-**TSb**, induce geometrical changes when compared to activated complexes (***R***)-**TSa** and (***S***)-**TSa**. For example, the proton in the transfer is more shifted from the carbon in the cyclohexene oxide part toward the amide nitrogen (C2–H1: 1.33 Å, N1–H1: 1.46 Å in (***R***)-**TSb** and (***S***)-**TSb**), than in (***R***)-**TSa** and (***S***)-**TSa** (C2–H1: 1.30 Å; N1–H1: 1.50 Å, respectively); the coordination of lithium (Li1) to the amide nitrogen (N1) is also slightly longer (0.05–0.07 Å), and the Li1–Li2 distance is increased (0.18–0.20 Å). At the B3LYP/6-31G(d) level of theory, the difference in potential energy between (***S***)-**TSa** and (***R***)-**TSa** was 0.66 kcal mol^{-1} favoring the formation of (*S*)-product. The changed orientation of the imidazole rings in (***S***)-**TSb** and (***R***)-**TSb** led to small increases of the activation energies (0.4 and 0.69 kcal mol^{-1}) when compared to (***S***)-**TSa** and (***R***)-**TSa**, respectively.

The potential energy difference between the two most stable activated complexes at the B3LYP/6-31G(d) level of theory corresponds to an enantiomeric excess of the (*S*)-enantiomer of 51% at 298 K (Table 2). The calculated Gibbs free energy difference between the two most stable activated complexes was 0.063 kcal mol^{-1} at 298 K, which corresponds to a calculated enantiomeric excess of the (*S*)-enantiomer of only 5%. Thus, the observed favored enantiomer is also the one that is predicted by the calculations although the prediction is far from being quantitative.

Activated complexes, with the coordination between the lithium and the nitrogen in the pyrrolidine ring broken,

Table 2. Calculated energy differences in kcal mol^{-1} between the most stable diastereoisomeric activated complexes at the B3LYP/6-31G(d), together with calculated and experimental enantiomeric excesses

Solvent	ΔE_{Calcd}[a]	ΔG_{Calcd}[b]	ΔG_{Exp}[c]	Ee_{Calcd}[d]	Ee_{Exp}
None	0.66			51(*S*)	
THF	0.73			56(*S*)	
None		0.063		5(*S*)	
THF		0.51		41(*S*)	
THF			2.30		96

[a] Potential energy difference between the two most stable TSs.
[b] Calculated Gibbs free energy differences between the two most stable TSs at 298 K.
[c] Experimental Gibbs free energy difference at 293 K calculated from the experimental ee.
[d] Enantiomeric excesses calculated from the potential energy difference between the two most stable TSs at 298 K.

were also investigated but were found to be 14–24 kcal mol^{-1} less stable than (***R***)-**TSa** at the B3LYP/6-31 + G(d)//PM3 level of theory and therefore not optimized further.

Monosolvation by THF of the lithium coordinating the epoxide oxygen in the activated complexes leads to stabilization by 1.7–4.9 kcal mol^{-1} at the PM3 level of theory. Monosolvation of the second lithium (Li2), which coordinates the nitrogen in the pyrrolidine ring in the activated complex of the mixed dimer, results in destabilization at the PM3 level of theory of the activated complexes by a few kcal mol^{-1}. Therefore, further solvation at this position was not considered.

The two most stable monosolvated activated complexes found at the B3LYP/6-31 + G(d)//PM3 level of theory were further optimized at the B3LYP/6-31G(d) level of theory.[22–24] A major structural difference caused by THF-solvation is that the bonds between lithium (Li1) and amide nitrogen (N1) are broken in (***R***)-**TS·THF** (3.79 Å) and (***S***)-**TS·THF** (3.72 Å), compared to their unsolvated counter parts (***R***)-**TSa** and (***S***)-**TSa** (2.14 Å).

The major differences between the activated complexes (***R***)-**TS·THF** and (***S***)-**TS·THF** comes from the differences in Li1–C3 and Li1–N2 bond lengths due to the orientation of the imidazole ring (Fig. 4). In (***R***)-**TS·THF**, the oxygen-coordinated lithium (Li1) is coordinated to a carbon (C3) in the imidazole ring, while in (***S***)-**TS·THF**, the lithium (Li1) is coordinated to the nitrogen (N2). The lithium coordination to the epoxide oxygen (O1) is also longer (0.04–0.05 Å) than in the unsolvated activated complexes due to the THF solvation.

The potential energy difference between the activated complexes (***R***)-**TS·THF** and (***S***)-**TS·THF** was 0.73 kcal mol^{-1} in favor of forming (*S*)-products at the B3LYP/6-31G(d) level of theory. The potential energy difference between the most stable activated complexes corresponds to an enantiomeric excess of 56% at 298 K. The calculated Gibbs free energy difference between the two most stable activated complexes was 0.51 kcal mol^{-1}, which corresponds to a calculated enantiomeric excess of the (*S*)-enantiomer of 41% (Table 2).

The energy difference between the geometry optimized activated complexes at the B3LYP/6-31G(d) predicts the (*S*)-allylic lithium alkoxide as the main product in the deprotonation of cyclohexene oxide. The theoretically derived enantiomeric excess was 51% for the unsolvated and 55% for the THF solvated activated complexes. Thus, the predicted values are lower than the experimentally observed ee of 96%.

4. Conclusion

The composition of the rate-limiting activated complex in the deprotonation of cyclohexene oxide by mixed dimer **5** has been determined using kinetics. Our results show that diastereoisomeric activated complexes are not only built from one molecule of the chiral lithium amide and one molecule of epoxide, but that the transition state also contains one molecule of the bulk base. Calculations correctly predicted the (*S*)-allylic alcohol as the major product in accordance with the experimental

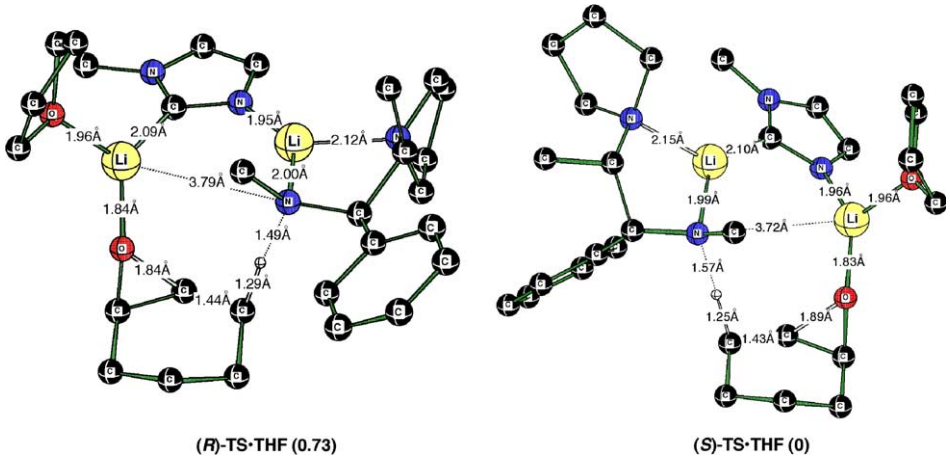

Figure 4. Optimized THF-solvated activated complexes at B3LYP/6-31G(d) level of theory. Relative energies in kcal mol^{-1} are shown in parentheses. Hydrogens are omitted for clarity.

result. These findings have implications for the use of mixed dimers in design of stereoselective deprotonation systems.

5. Experimental

5.1. General

Reaction vessels and syringes dried in a vacuum oven (50 °C) overnight. Transfers of reagents were performed with gas-tight syringes in nitrogen atmosphere. THF was distilled from sodium benzophenone ketyl in a nitrogen atmosphere and stored over molecular sieves (4 Å) in septum sealed vials in a glove box (Mecaplex GB 80 equipped with a gas purification system that removes oxygen and water). A stock solution (2.0 M) of cyclohexene oxide (distilled from calcium hydride) in THF was prepared inside the glove box. 1-Hexanol was used as a standard in the GC-analysis; a stock solution (3.40 mM) of 1-hexanol (distilled from calcium hydride) in carbon tetrachloride (distilled from calcium chloride) was prepared. The concentration of *n*-butyllithium was determined by a double Gilman titration.[9]

5.2. Gas chromatography analysis

Gas chromatography analyses were performed on a Varian 3400 chromatograph equipped with an 8200 Cx auto sampler and a flame ionization detector (FID). For the separation, an achiral DBWX-30W column (30 m, 0.25 μm) from Varian Inc. was used with hydrogen as the carrier gas (2 mL min^{-1}). Reaction samples (1.0 μL) were introduced onto the column via a split injector (split flow 15 mL min^{-1}) and the components separated using a temperature program. Initially the temperature was held at 80 °C for 2 min and then for a further 2 min increased to 120 °C. The injector temperature was 225 °C while the detector was held at 250 °C.

Gas chromatography response factors for **2** and **4** were determined, using 1-hexanol as a reference, to be 1.01and 0.85, respectively. The enantiomeric excesses of **4** were measured using a Chrompack Chirasil-CB Dex (30 m, 0.25) at 95 °C. t_R (*S*)-**4** = 6.85 min, t_R (*R*)-**4** = 7.30 min.

The reproducibility of the GC-analyses procedure was investigated by analysis of a reaction sample of the (*S*)- and (*R*)-allylic alcohol [93% ee of (*S*)]. Seventeen injections gave an average value of 93.3% with 2σ equal to 0.2%. The enantiomeric excess of the (*S*)-allylic alcohol was monitored during the conversion of the epoxide while the ee was found to be consistently within experimental error (95.8 ± 0.3%).

5.3. Typical kinetic procedure

Amine (1*R*,2*S*)-*N*-methyl-1-phenyl-2-pyrrolidinyl-propanamine[9] (21.8 μL, 0.1 mmol) and 1-methylimidazole (50 μL, 0.1 mmol, 2 M in THF) were dissolved in THF (796 μL) in a reaction vessel inside a glove box, transferred out of the glove box and *n*-butyllithium (82.0 μL, 0.2 mmol, 2.44 M in hexanes) then added under a nitrogen atmosphere. The yellow reaction solution was allowed to equilibrate at 20.00 ± 0.05 °C for 10 min in a thermostat. The reaction was started by the addition of cyclohexene oxide **2** (50 μL, 0.1 mmol, 2.0 M) with samples (50 μL) withdrawn at approximately 3 min intervals from the reaction vessel and quenched in hydrochloric acid solution (100 μL, 0.6 M saturated with sodium chloride). Compounds **2** and **4** were extracted with carbon tetrachloride (500 L) containing the standard 1-hexanol (3.40 mM). The liquid phases were separated by centrifugation and the organic phase transferred to a vial and analyzed by capillary gas chromatography.

The quantitative transfer of **2** and **4** from the aqueous phase to the carbon tetrachloride phase during the workup was determined as follows: solutions of **2** and **4** in THF with compositions similar to those in the kinetic experiments were prepared. Samples (50 μL) were withdrawn and added to solutions of carbon tetrachloride (500 μL) containing 1-hexanol (3.16 mM). Other samples (50 μL) of solutions of **2** and **4** were added to solutions of hydrochloric acid (100 μL, 0.6 M saturated with sodium chloride). The latter mixtures were extracted with solutions of carbon tetrachloride (500 μL) containing 1-hexanol (3.16 mM). After separation by centrifugation, the organic layers were transferred to vials. The samples from the two types of preparations were analyzed with capillary gas chromatography. The concentration ratios of epoxide **2** and allylic alcohol **4** to 1-hexanol determined for the two types of preparations were found to be within 0.5% of the average value, respectively.

The concentration of **4** was measured for about the first 0.5% of conversion of **2**. Initial rates were usually reproduced within 2% of the average values, respectively.

5.4. Computational details

All activated complexes were optimized at the PM3 level of theory using the option HHon.[10–14] All activated complexes were verified as first order saddle points on the potential energy surface (PES) by using the frequencies obtained from the force constant matrix and by visualization of the imaginary frequency at the PM3. The most stable activated complexes at the B3LYP/6-31 + G(d)//PM3 level of theory were further optimized at the B3LYP/6-31G(d) level of theory.[22–24] All DFT calculations were performed by GAUSSIAN 98.[25]

The most stable activated complexes [three leading to the (*R*)- and three leading to (*S*)-product] at the B3LYP/6-31 + G(d)//PM3 level of theory were then further geometrically optimized at B3LYP/6-31G, followed by geometry optimization at the B3LYP/6-31G(d) level of theory. Different conformers of the activated complexes

were investigated by structure modifications. These modifications were performed by altering the orientation of the imidazole ring, having either an (*R*)- or (*S*)-configuration on the abstracting amide nitrogen, by rotation of the phenyl group, by breakage of the coordination between the lithium and the nitrogen in the pyrrolidine ring. Different conformers of the cyclohexene oxide and pyrrolidine ring were also investigated. In order to model how the solvent, THF, influences the structure of the activated complexes, the most stable activated complexes were optimized at the PM3, and B3LYP/6-31G(d) level of theory, where one or two lithium atoms in the activated complexes were specifically solvated with one or two THF molecules. Altogether, about 276 unsolvated, mono-, and di-THF solvated activated complexes were calculated at the PM3 level of theory.

Acknowledgements

We thank the Swedish Research Council for financial support and the National Supercomputer Centre in Linköping, Sweden, for computational resources.

References and notes

1. O'Brien, P. *J. Chem. Soc., Perkin Trans. 1* **1998**, 1439–1457.
2. Asami, M.; Suga, T.; Honda, K.; Inoue, S. *Tetrahedron Lett.* **1997**, *37*, 6425–6428.
3. Bertilsson, S. K.; Södergren, M. J.; Andersson, P. G. *J. Org. Chem.* **2002**, *67*, 1567–1573.
4. Pettersen, D.; Amedjkouh, M.; Ahlberg, P. *Tetrahedron* **2002**, *58*, 4669–4673.
5. Amedjkouh, M.; Pettersen, D.; Nilsson Lill, S. O.; Davidsson, Ö.; Ahlberg, P. *Chem. Eur. J.* **2001**, *7*, 4368–4377.
6. Amedjkouh, M. *Tetrahedron: Asymmetry* **2004**, *15*, 573–746.
7. Olsson, R. I.; Ahlberg, P. *Tetrahedron: Asymmetry* **1999**, *10*, 3991–3998.
8. Collum, D. B. *Acc. Chem. Res.* **1993**, *26*, 227–234.
9. Pettersen, D.; Amedjkouh, M.; Nilsson Lill, S. O.; Dahlén, K.; Ahlberg, P. *J. Chem. Soc., Perkin Trans. 2* **2001**, *9*, 1654–1661.
10. Anders, E.; Koch, R.; Freunscht, P. *J. Comput. Chem.* **1993**, *14*, 1301–1312.
11. Stewart, J. J. P. *J. Comput. Chem.* **1989**, *10*, 209–220.
12. Hehre, W. J.; Deppmeier, B. J.; Driessen, A. J.; Johnson, J. A.; Klunzinger, P. E.; Lou, L.; Yu, J.; Baker, J.; Carpenter, J. E.; Dixon, R. W.; Fielder, S. S.; Johnson, H. C.; Kahn, S. D.; Leonard, J. M.; Pietro, W. J. *Spartan v. 5.0.1*; Wavefunction: Irvine, CA, 1997.
13. Csonka, G. I.; Ángyán, J. G. *J. Mol. Struct.* **1997**, *393*, 31–38.
14. Csonka, G. I. *J. Comput. Chem.* **1993**, *14*, 895–898.
15. Hilmersson, G.; Arvidsson, P. I.; Davidsson, Ö.; Håkansson, M. *J. Am. Chem. Soc.* **1998**, *120*, 8143–8149.
16. Abbotto, A.; Streitwieser, A.; Schleyer, P. v. R. *J. Am. Chem. Soc.* **1997**, *119*, 11255–11268.
17. Thummel, R. P.; Rickborn, B. *J. Am. Chem. Soc.* **1970**, *92*, 2064–2067.
18. Morgan, K. M.; Gajewski, J. J. *J. Org. Chem.* **1996**, *61*, 820–821.
19. Manuscript (*in preparation*).
20. Becke, A. D. *J. Chem. Phys.* **1993**, *98*, 1372–1377.
21. Lee, C.; Yang, W.; Parr, R. G. *Phys. Rev. B: Condens. Matter* **1988**, *37*, 785–789.
22. Hehre, W. J.; Ditchfield, R.; Pople, J. A. *J. Chem. Phys.* **1972**, *56*, 2257–2261.
23. Frisch, M. J.; Pople, J. A.; Binkley, J. S. *J. Chem. Phys.* **1984**, *80*, 3265–3269.
24. Hariharan, P. C.; Pople, J. A. *Theor. Chim. Acta* **1973**, *28*, 213–222.
25. GAUSSIAN98; Gaussian: Pittsburgh, PA.